Voiding and Drop Test Performance of Lead-Free Low Melting and Medium Melting Mixed Alloy BGA Assembly

Yan Liu, Joanna Keck, Erin Page, and Ning-Cheng Lee
Indium Corporation
Clinton, NY

Abstract
Low melting 57Bi42Sn1Ag (BiSnAg) was explored for replacing SAC solders as a low-cost solution. In this study, BGAs with SAC105, SAC305, and BiSnAg balls were assembled with SAC105, SAC305 or 57Bi42Sn1Ag solder paste. Joint mechanical strength, drop test performance, and voiding performance were evaluated against the reflow profile. SnPb was included as a control. The findings are as follows: (1) The microstructure of solder joints showed that, among all of the combinations, only BiSnAg-105 LT and BiSnAg-305 LT exhibited well-distinguishable alloy regions. For SAC-BiSnAg systems, Sn-dendrites were noticeable at LT, while Ag3Sn needles developed at HT. The joints were homogeneous for the rest of the combinations. (2) In the shear test, combinations involving BiSnAg solder were brittle, regardless of the Bi alloy location and reflow profile, as evidenced by stress-strain curves and morphology of the ruptured surface. The strong influence of Bi on the rupture site may have been caused by the stiffening effect of solder due to the homogenized presence of Bi in the joint. With the stiffened solder, the brittle IMC interface became the weakest link upon shearing, although the brittle BiSn crystalline structure also contributed to the rupture. (3) In the drop test, all Bi-containing solder joints performed poorly compared with Bi-free systems, which was consistent with shear test results. Drop numbers increased with increasing elongation at break of solder bumps as measured in the shear test. (4) Voiding was affected by flux chemistry and reduced by low alloy homogenization temperatures and solid top factors, but was increased by low surface tension factor, melting sequence factor, overheating factor and wide pasty range factor. Compared to SAC or SnPb systems, the BiSnAg system is low in voiding if reflowed at LT. In this study, voiding had an insignificant effect on shear strength and drop test performance.

Introduction
Driven by low-cost consideration, low temperature soldering for PCB assembly has the potential of reducing the cost of materials for components and boards, in addition to reducing the energy for reflow soldering. Among all options, 57Bi42Sn1Ag (BiSnAg) is one of the most notable choices due to its low melting temperature and promising mechanical property. Because SAC alloys are the prevailing solders in use in the industry, adopting BiSnAg inevitably faces the challenge of mixed solder alloys, particularly in voiding and drop test performances. Although low melting assembly may be the primary focus, the possible impact of assembling BGAs with low melting alloy balls with SAC alloys should also be examined in order to assess the potential risk of mixed alloy situation. In this study, BGAs with SAC105, SAC305, or BiSnAg balls were assembled with SAC105, SAC305 or 57Bi42Sn1Ag solder paste. Joint mechanical strength, drop test performance, and voiding performance were evaluated against the reflow profile. Joints were also analyzed by using differential scanning calorimetry (DSC) and a scanning electron microscope (SEM) to identify the effect of melting behaviors and microstructures on those properties. 63Sn37Pb (SnPb) was used as a control for comparison.

Experiment
1. Materials
Solder sphere: 25 mils (635 μ) diameter, with BiSnAg, SAC105, SAC305, and SnPb alloy compositions
Solder powder: Type 3 powder, with BiSnAg, SAC105, SAC305, and SnPb alloy compositions
Solder paste no-clean fluxes: Company paste A for BiSnAg (88.75% metal load), Company Paste B for SAC (88.5% metal load), and Company Paste C for SnPb (88.5% metal load)
Water soluble flux for BGA bumping: Company Flux D

2. Reflow Profiles
Three reflow profiles were used in this study: (1) low temperature tent profile (LT), with a peak temperature of 176°C, (2) SnPb medium temperature tent profile (MT), with a peak temperature of 216°C, and (3) high temperature tent profile (HT), with a peak temperature of 236°C.

3. Voiding and Elemental Mapping
1). BGA substrate with 24x24 pads, 40 mils (1.02 mm) pitch, and 25 mils (635 μ) Cu pad diameter, as shown in Fig. 1.
2). A dummy BGA was prepared by first printing water soluble flux onto a BGA substrate using a stencil that was 3.5 mils (89 μ) thick with a 25 mils (635 μ) aperture. Next, a solder ball with a diameter of 25 mils (635 μ) was placed. This device was then reflowed with a designated profile to form a dummy BGA, followed by water cleaning to remove flux residue and drying.
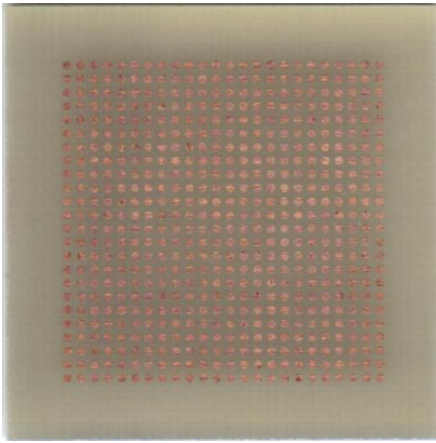
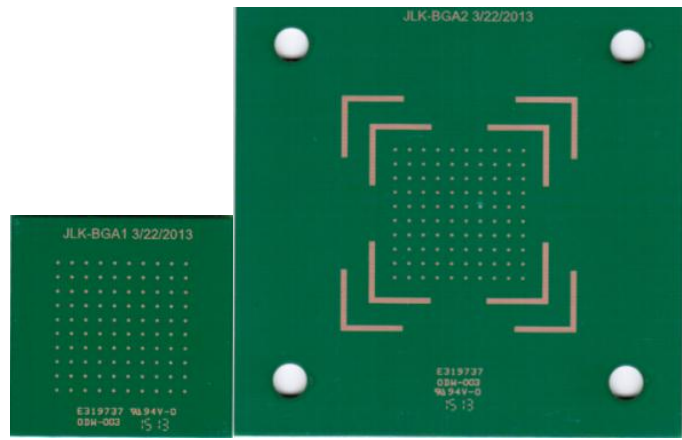**Figure 1** BGA coupon for voiding and elemental mapping study.

Figure 2 Test coupons used in drop test.

3). The no-clean solder paste in this study was printed onto a fresh BGA substrate using the same stencil.

4). The dummy BGA made earlier was placed onto the BGA substrate printed with solder paste.

5). The sandwiched device was reflowed using a designated profile under nitrogen.

6). Voiding was examined with X-ray for all joints.

7). The device was then cross-sectioned for energy-dispersive X-ray spectroscopy (EDS) elemental mapping on the solder joints.

4. DSC

1). A designated no-clean solder paste was printed onto a ceramic coupon using the same stencil (3.5 mils thickness and 25 mils aperture). One printed dot was then scraped up with a razor.

2). A 25 mils diameter solder sphere with a designated solder alloy was picked up with fine tip tweezers. The sphere on the tweezers was then scraped against the paste on razor's edge until all the paste was picked up by the sphere, as verified under the optical microscope.

3). The sphere with paste was then transferred to a DSC sample cell for DSC study using a heat rate of 10°C/minute up to 300°C.

5. Drop Test

Coupon JLK-BGA1 (see Fig. 2, left) was used for a simulated BGA, as described in the Voiding section. Coupon JLK-BGA2 (see Fig. 2, right) was used for simulating a PCB substrate for the drop test. Both coupons are SMD OSP finished Cu pad. In order to intensify the test condition to reduce the number of drops needed to fail, the I/O density was reduced, with a pad diameter of 25 mils, and a pitch of 100 mils, and total I/O 100. The process on sample preparation is similar to that of the voiding study.

The BGA assembly was mounted onto the steel block of drop testing equipment, as shown in Fig. 3.
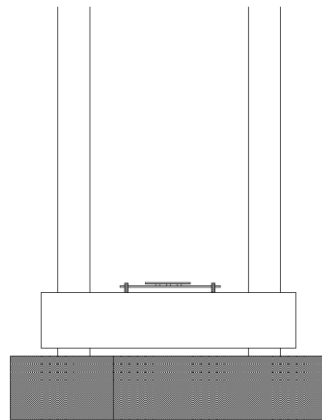

Figure 3 Schematic of drop tester setup.

Table 1 Combination of solder alloys and reflow profiles.

Alloy		Profile		
Paste	Ball	LT	HT	MT
BiSnAg	BiSnAg	Y	-	-

BiSnAg	BiSnAg	-	Y	-
BiSnAg	105	Y	-	-
BiSnAg	105	-	Y	-
BiSnAg	305	Y	-	-
BiSnAg	305	-	Y	-
105	BiSnAg	Y	-	-
105	BiSnAg	-	Y	-
105	105	-	Y	-
105	305	-	Y	-
305	BiSnAg	Y	-	-
305	BiSnAg	-	Y	-
305	105	-	Y	-
305	305	-	Y	-
SnPb	SnPb	-	-	Y

The height used for the drop test was 0.25 meter. For each test condition, 5-10 simulated BGA assemblies were used. Failure was assessed by the full detachment of BGA from PCB substrate. **Figure 4** DSC of first heating thermographs of various alloy combinations.
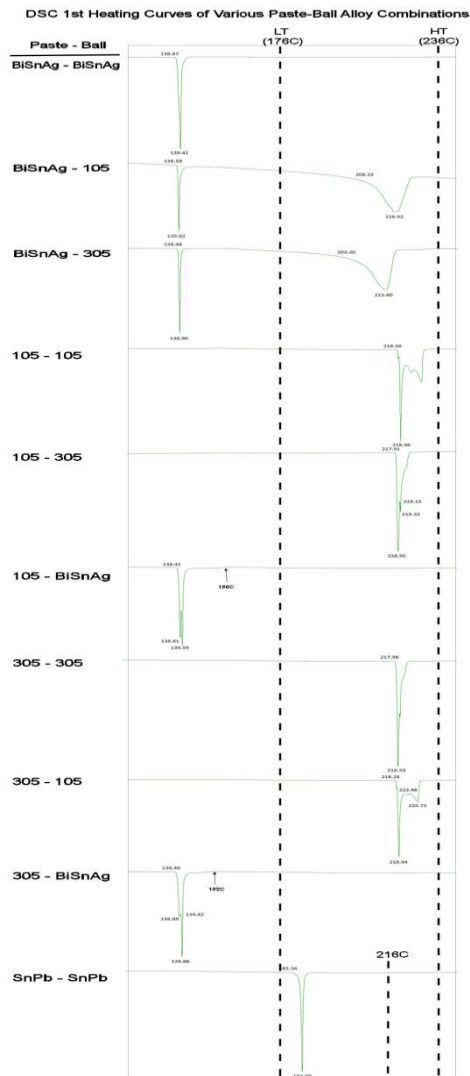
Figure 4 DSC of first heating thermographs of various alloy combinations.
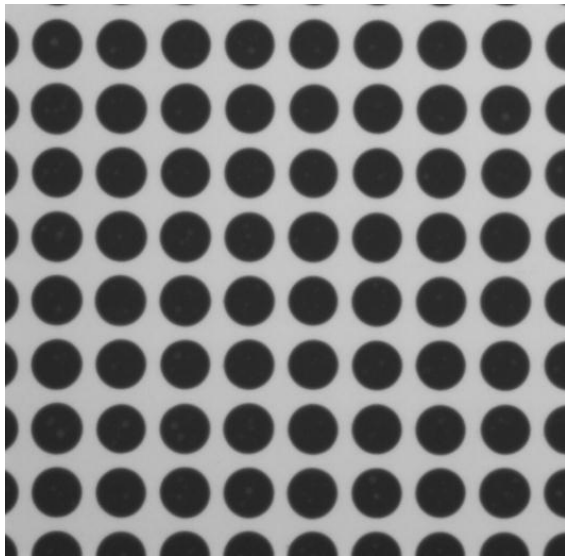
Figure 5 X-ray of BiSnAg-BiSnAg LT BGA joints.
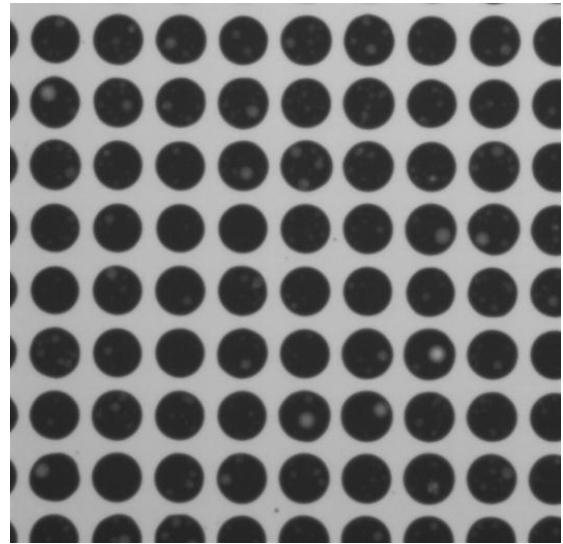
Figure 6 X-ray of BiSnAg-BiSnAg HT BGA joints.

6. Shear Test
The shear strength of solder bumps prepared by reflowing spheres mounted with solder paste on coupon JLK-BGA1 was determined, with stress-strain curves recorded. For each system, 20-25 bumps were tested.

7. DOE
The DOE on combinations of alloys and profiles are shown in Table 1. Unless otherwise specified, the combination of alloys and profiles in this study are represented as paste-ball profiles, such as BiSnAg-105 HT.

Results
1. DSC
Within the BGA solder joints, calculated results show that a 10% volume fraction of solder came from the solder paste, and 90% came from the sphere. This volume fraction relationship is also applicable to the DSC sample.

The DSC first-heating thermographs of various alloy combinations are shown in Fig. 4. For paste-ball combinations reflowed with a LT profile, BiSnAg-BiSnAg was fully melted; SAC-SAC and SnPb-SnPb were not melted at all. BiSnAg-SAC showed that a significant portion of solder was not melted. This was attributed to the dominant volume of the high melting SAC ball. However, SAC-BiSnAg showed full melting behavior, where SAC105-BiSnAg completely melted at 156°C, while SAC305-BiSnAg completely melted at 152°C. The full melting behavior of SAC-BiSnAg can be attributed to the dominant solder volume of the BiSnAg ball. At temperatures above 138°C, the volume-dominant BiSnAg ball melted first, then continued to dissolve the SAC powder until all SAC powder was alloyed with BiSnAg from152-156°C.

When reflowed at a HT profile, all alloys melted as expected.

2. Voiding
The voiding performance of various alloy combinations and reflow profiles were determined by X-ray, as shown in Fig. 5 and Fig. 6 for BiSnAg-BiSnAg systems. The results are shown in Table 2.

Fig. 5 and Fig. 6 show the effects of reflow temperatures on the voiding of BiSnAg-BiSnAg systems, with high reflow temperatures (HT) resulting in higher voiding.

This can be attributed to the overheating factor [1], which means that at higher reflow temperatures, flux outgassed more due to more vaporization and thermal decomposition, thus resulting in more voiding.

Fig . 7 shows the effect of the reflow temperature on the voiding of various alloy and profile combinations. Among the SAC-SAC systems, 105-305 HT exhibited the highest voiding, mainly attributed to the melting sequence factor [1], where the top SAC305 ball melted earlier than SAC105 paste, thus allowing more entrapment of outgassing in the top ball area. SnPb-SnPb is higher in voiding than most of the SAC-SAC systems mainly due to the low surface tension factor [1].

Table 2 Voiding performance of various alloy combinations.

Paste/Ball Profile	# Voids			Voiding (Area %)		
	Avg	STD DEV	Max	Avg	STD DEV	Max Void
BiSnAg/BiSnAgLT	0.99	0.65	3.00	1.36	1.14	6.72
BiSnAg/BiSnAgHT	1.38	0.91	4.00	2.67	2.85	31.65
BiSnAg/105LT	0.95	0.70	3.00	0.57	0.42	2.39
BiSnAg/105HT	1.88	0.94	5.00	5.55	4.05	20.97
BiSnAg/305LT	1.17	0.76	5.00	0.74	0.49	3.49
BiSnAg/305HT	2.17	1.00	5.00	5.90	4.11	28.34
105/105HT	0.59	0.59	2.00	0.51	0.58	2.99
105/305HT	1.81	0.88	5.00	3.57	2.02	11.92
305/305HT	1.35	0.92	5.00	1.72	1.44	7.61
305/105HT	1.45	1.06	5.00	1.45	1.21	6.48
SnPb/SnPb	1.95	-	-	3.48	-	9.22
305/BiSnAgLT	0.34	0.48	2.00	0.22	0.34	2.73
305/BiSnAgHT	0.25	0.45	2.00	0.19	0.42	5.61
105/BiSnAgLT	0.31	0.48	2.00	0.19	0.30	1.54
105/BiSnAgHT	0.32	0.51	2.00	0.25	0.48	4.14
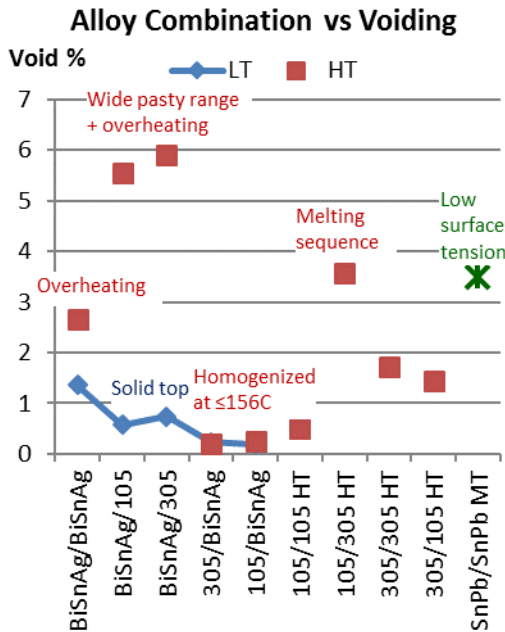
Figure 7 Effect of reflow temperature on voiding for various alloy combinations.
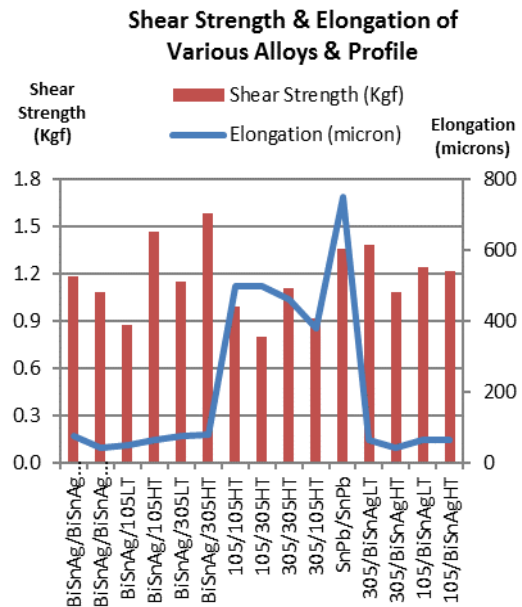
Figure 8 Effect of alloy combination and profile on bump shear strength and elongation at break.

The surface tension of SnPb and SAC solder is 0.51 and 0.57 N/m, respectively [2]. This lower surface tension exerted less restrictive force on the expansion of voids thus forming larger voids [1].

For the BiSnAg-105 and BiSnAg-305 systems, the higher voiding of HT than LT are attributed to both the overheating factor and a lack of the solid top factor [1]. The solid top factor can be seen in Fig. 4, where both SAC105 and SAC305 balls remained solid during the LT process. Since volatiles could not get into the solid top at reflow, the voiding would be lower. During the HT process, the top ball melted fully thus allowing the volatiles to enter to form a void. For SAC-BiSnAg cases, no significant effect of reflow temperatures can be discerned, mainly due to the nature of the flux used for SAC solder paste.

The lower voiding of SAC-BiSnAg compared to BiSnAg-SAC was partly due to the SAC-BiSnAg solder being homogenized at a temperature below 156°C and all of the flux was expelled from the interior of solder joint. Although the melting sequence of SAC-BiSnAg was prone to have more voiding due to the early melting of the top BiSnAg ball, no volatile was released from the flux for SAC paste at this low temperature (156°C). The lower voiding of SAC-BiSnAg was also due to the lower voiding of flux chemistry used for SAC paste when compared to the BiSnAg paste in the BiSnAg-SAC system or the BiSnAg-BiSnAg system.

For the LT process, the BiSnAg-SAC system is lower in voiding than BiSnAg-BiSnAg, due to the solid top factor as in the previous case. For the HT process, a wide pasty range factor dictated the voiding [1]. The pasty range is 79°C (138°C to 217°C) for BiSnAg-105, and 76°C (138°C to 214°C) for BiSnAg-305, as shown in Fig. 4. Here, the solder with a wide pasty range was more prone to entrap volatiles, thus forming more voiding. BiSnAg-BiSnAg melted at a single melting point (see Fig. 4).

Overall, voiding was affected by flux chemistry, reduced by a low alloy homogenization temperature and a solid top factor, but was increased by a low surface tension factor, melting sequence factor, overheating factor, and wide pasty range factor. Compared with SAC or SnPb systems, the BiSnAg system in general is low in voiding if reflowed at LT.

3. Elemental Mapping

The solder joints of various alloy and reflow profile combinations were examined with EDS for elemental mapping, and the images are shown in Appendix A. Among all of the combinations, only BiSnAg-105 LT and BiSnAg-305 LT exhibit well-distinguished alloy regions. These two combinations correlated well with the DSC data shown in Fig. 4, where the SAC balls remain solid when reflowed with LT profile. When reflowed at HT, the alloy-zones disappeared, but the Bi-rich micro-regions can still be discernible.

Table 3 Shearing stress-strain curves of solder bumps with various alloys and reflow profile combinations (Paste-Ball Profile).

BiSnAg-BiSnAg LT	BiSnAg-305 HT	SnPb-SnPb MT
BiSnAg-BiSnAg HT	**105-105 HT**	**305-BiSnAg LT**
BiSnAg-105 LT	**105-305 HT**	**305-BiSnAg HT**
BiSnAg-105 HT	**305-305 HT**	**105-BiSnAg LT**
BiSnAg-305 LT	**305-105 HT**	**105-BiSnAg HT**
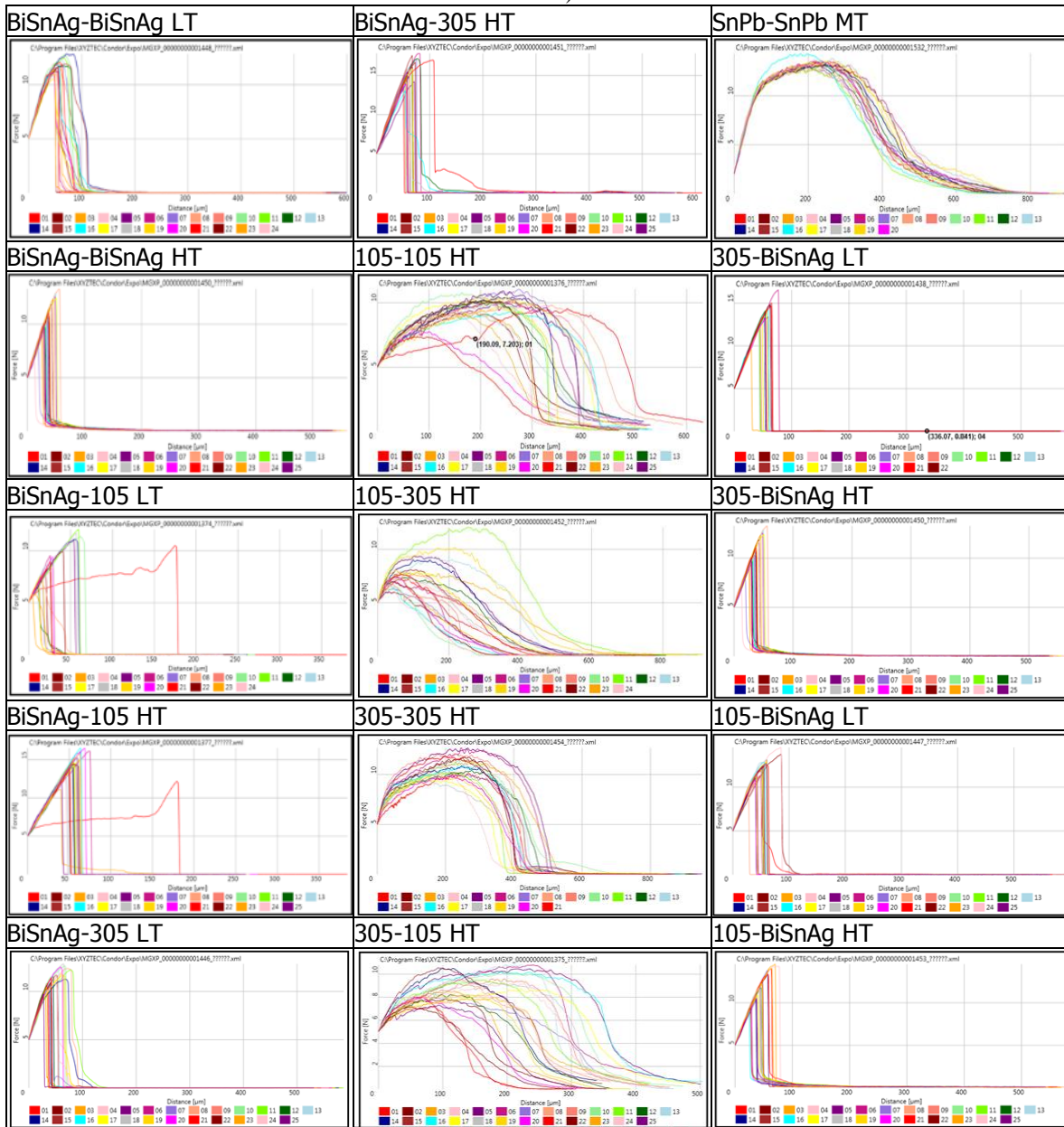
105-BiSnAg LT and 305-BiSnAg LT exhibit a nearly homogeneous elemental distribution, with tin-dendrites easily distinguishable. When reflowed at HT, those tin-dendrites vanished, while well-defined Ag-rich needle structures emerged from the solder-pad interface, presumably due to the Ag3Sn IMC formation. The Ag-rich needle structures are also discernible in BiSnAg-BiSnAg LT and HT systems. The development of Ag-rich needle structures can be attributed to the extended liquid state of solder at reflow, which allowed significant diffusion of Ag to form IMC at interface, as reflected by the DSC curves.

4. Shear Test

The shearing stress-strain curves and data of solder bumps of various alloys and reflow profile combinations are shown in Table 3 and Table 4.

In Table 3, the curve shapes indicate that all combinations involving BiSnAg solder are brittle, regardless of the Bi alloy location and reflow profile. The average value of elongation at break in Table 4 also shows Bi-containing systems are below 80 microns, while those for the non-Bi-containing systems are above 380 microns.

Table 4 Shearing stress-strain data of solder bumps with various alloys and reflow profile combinations (Paste-Ball Profile).

Paste-Ball Profile	Elongation at Break (micron)				Shear Strength (Kgf)				
	Min.	Avg.	Max.	Tail	Min.	Avg.	Max.	Range	STDEV
BiSnAg-BiSnAg LT	50	75	115	170	1.07	1.19	1.31	0.24	0.06
BiSnAg-BiSnAg HT	15	40	55	100	0.74	1.09	1.35	0.62	0.15
BiSnAg-105 LT	15	50	175	175	0.50	0.88	1.23	0.73	0.21
BiSnAg-105 HT	43	65	180	180	1.13	1.47	1.68	0.55	0.14
BiSnAg-305 LT	35	75	140	140	0.99	1.15	1.31	0.32	0.09
BiSnAg-305 HT	50	80	110	220	1.33	1.59	1.82	0.49	0.13
105-105 HT	400	500	510	700	0.75	0.99	1.13	0.38	0.09
105-305 HT	300	500	700	700	0.61	0.80	1.23	0.62	0.14
305-305 HT	370	460	550	680	0.95	1.11	1.29	0.34	0.10
305-105 HT	250	380	500	500	0.73	0.91	1.10	0.37	0.12
SnPb-SnPb MT	700	750	800	800	1.30	1.36	1.46	0.16	0.04
305-BiSnAg LT	35	65	80	80	1.02	1.38	1.69	0.67	0.14
305-BiSnAg HT	15	40	55	100	0.74	1.09	1.35	0.62	0.15
105-BiSnAg LT	30	63	80	120	0.97	1.24	1.48	0.52	0.10
105-BiSnAg HT	25	63	80	200	0.90	1.21	1.48	0.58	0.16

The shear strength of solder materials appears to have no correlation with the solder bump composition, as seen in Fig. 8. Here, the shear strength of various alloys and profile combinations scattered between 0.8 and 1.6 Kgf. No significant trend can be discerned.

5. SEM Image of Sheared Bumps
On the other hand, SAC-SAC and SnPb-SnPb all failed in the bulk solder region, with ductile textures at the rupture surface.

After the bump shear test, the specimen fracture surface was examined for SEM analysis, with results shown in Table 5. Again, the images show that any combinations involving BiSnAg solder are brittle, regardless of the Bi alloy location and reflow profile.

On the other hand, SAC-SAC and SnPb-SnPb all failed in the bulk solder region, with ductile textures at the rupture surface.

In order to further elucidate the elemental composition of the brittle fracture surface, the close-up picture and EDS analysis were conducted on several systems. Fig. 9 shows the ruptured pad surface of BiSnAg-BiSnAg LT at 1000X. Region A shows a crystalline structure, while region B shows a flat texture. EDS analysis results in Table 7 shows the crystalline region A is mainly 58Bi42Sn solder, while the flat region B is mainly Cu6Sn5. The occurrence of rupture at the solder-pad interface indicates that the brittle CuSn IMC is the weakest link of joint. The significant presence of the crystalline phase indicates that the brittle nature of the crystalline structure also contributed to the rupture.
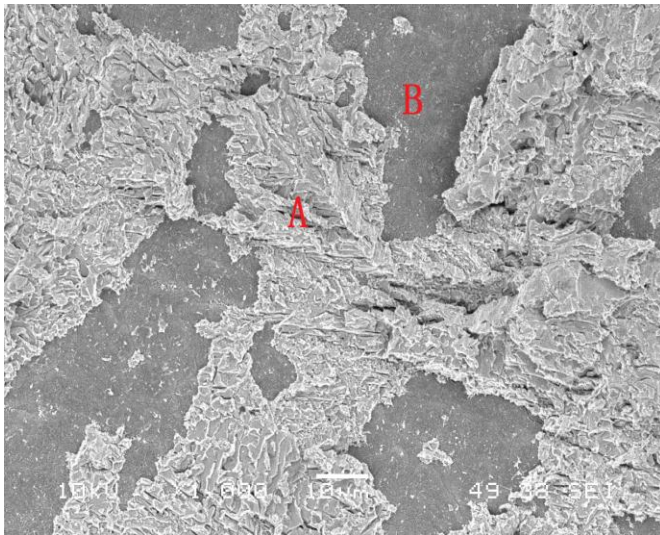
Figure 9 SEM 1000X picture of BiSnAG-BiSnAg LT ruptured surface on pad.
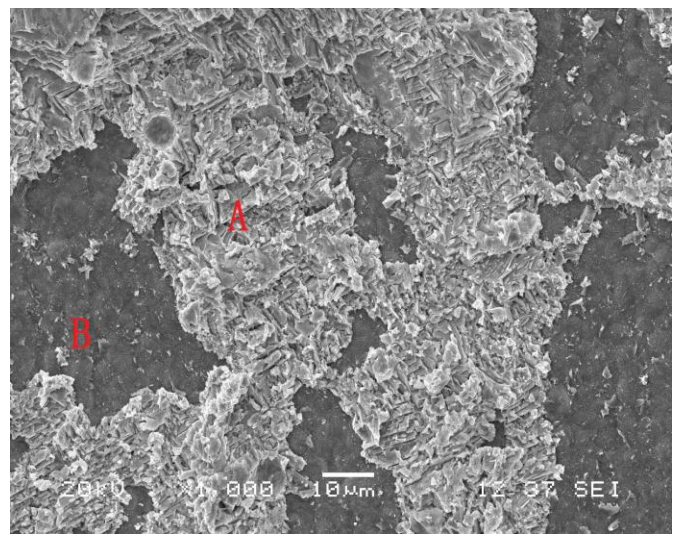
Figure 10 SEM 1000X picture of BiSnAG-BiSnAg HT ruptured surface on pad.

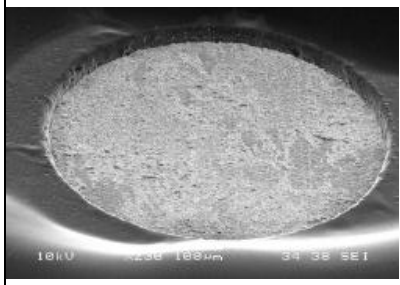**Table 5** SEM images of sheared solder bumps for various alloy and profile combinations.
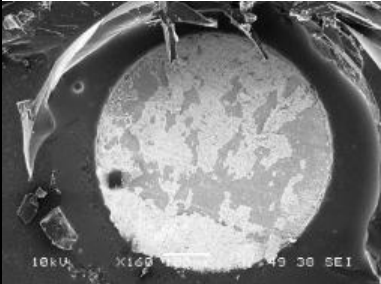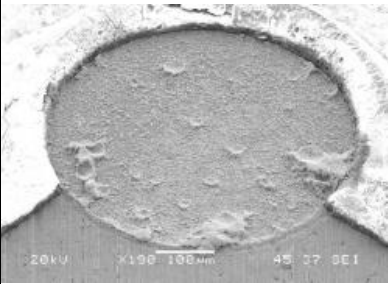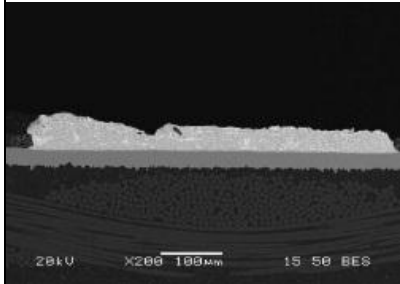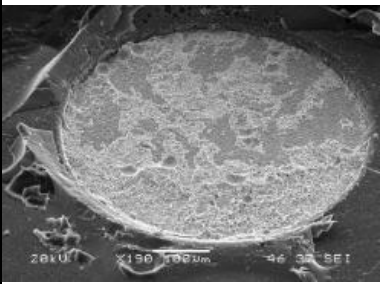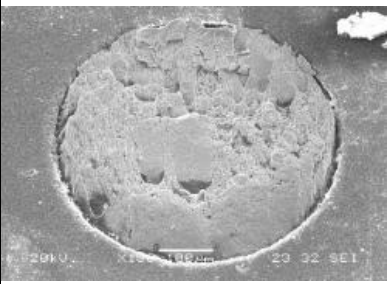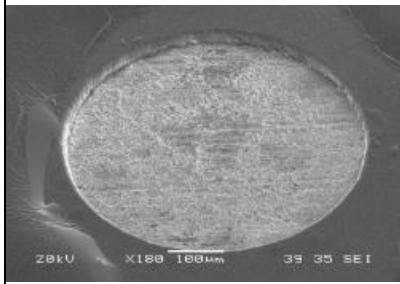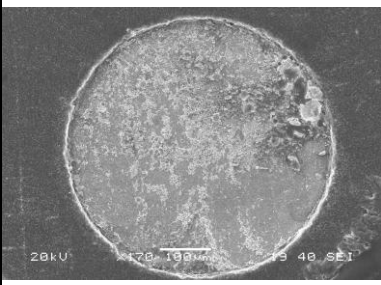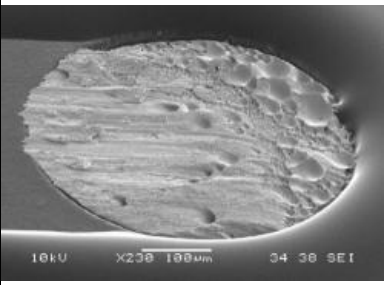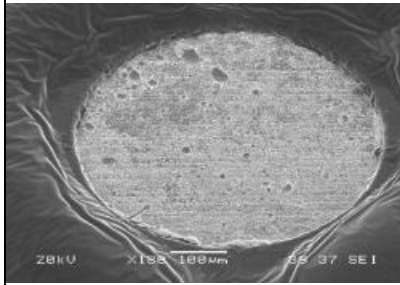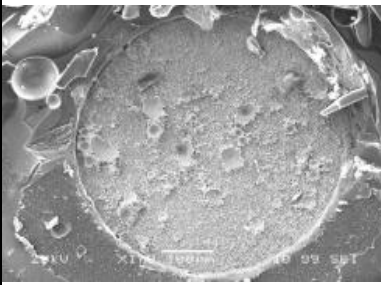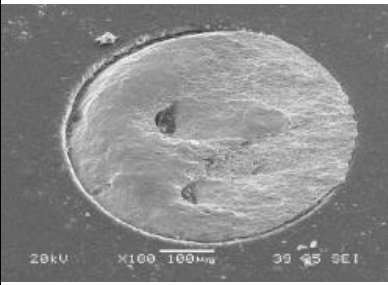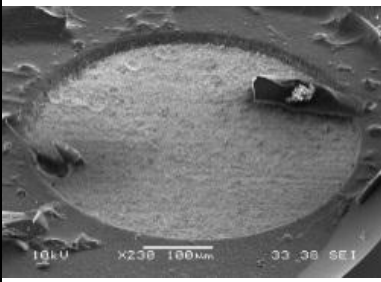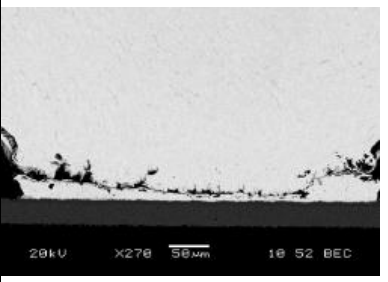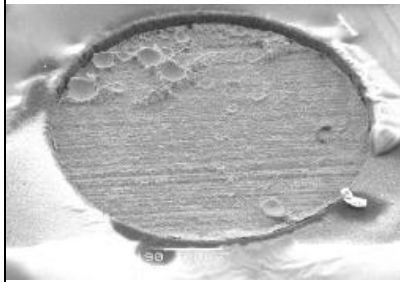
BiSnAg-BiSnAg LT	BiSnAg-305 HT	SnPb-SnPb MT
BiSnAg-BiSnAg HT	105-105 HT	305-BiSnAg LT
BiSnAg-105 LT	105-305 HT	305-BiSnAg HT
BiSnAg-105 HT	305-305 HT	105-BiSnAg LT
BiSnAg-305 LT	305-105 HT	105-BiSnAg HT

Table 6 EDS analysis results on several brittle ruptured surface.

Paste-Ball Profile		Atomic %			Weight %		
		Cu	Sn	Bi	Cu	Sn	Bi
BiSnAg-BiSnAg LT	A	2.99	55.78	41.24	1.23	42.91	55.86
	B	47.86	43.59	8.55	30.41	51.73	17.86
BiSnAg-BiSnAg HT	A	10.27	57.11	32.61	4.58	47.58	47.84
	B	68.36	29.63	2.01	52.46	42.47	5.07
BiSnAg-105 LT	A	2.99	55.78	41.24	1.23	42.91	55.86
	B	56.62	37.88	5.51	38.92	48.63	12.45
BiSnAg-105 HT	A	No Bi-rich region found					
	B	61.32	35.66	3.03	44.48	48.31	7.22

Fig. 10 shows the ruptured pad surface of BiSnAg-BiSnAg HT at 1000X. Similar to Fig. 9, region A shows a crystalline structure, while region B shows a flat texture. EDS analysis results in Table 6 shows that the crystalline region A is mainly BiSn solder, while the flat region B may be mixed Cu6Sn5 and Cu3Sn. The effect of the higher reflow temperature appears to have some effect on the CuSn IMC structure, although the primary failure mode is still similar to that of LT profile.

Fig. 11 shows the ruptured pad surface of BiSnAg-105 LT at 1000X. The morphology is lower in local uniformity compared with BiSnAg-BiSnAg systems, although region A still shows a crystalline 58Bi42Sn structure, while region B shows a flat texture of CuSn IMC.

Fig. 12 shows the ruptured pad surface of BiSnAg-105 HT at 1000X. The morphology is rougher than the LT system, and only CuSn IMC is observed at the ruptured surface, as shown in Table 7. Apparently, a higher reflow temperature drove the rupture further toward the CuSn layer, presumably due to the formation of a thicker IMC layer than a lower reflow temperature.

It is interesting to note that although 90% of the solder joint volume was composed of solder ball material, all BiSnAg-SAC systems still failed at the solder-pad interface, while all SAC-SAC or SnPb-SnPb systems failed within the bulk solder. The strong influence of Bi on the rupture site may be caused by the stiffening effect of solder due to the homogenized presence of Bi in the joint. Because the solder body was stiffened, the brittle IMC interface became the weakest link upon shearing.

6. Drop Test

The results of the drop test are shown in Table 7. All Bi-containing systems failed at first drop. The rest of the systems failed, ranging from 3 to 39 drops. Besides solder joints were brittle with Bi incorporated, the sparse number of joints per BGA (see Fig. 2) further reduced the drop number to one. Among the failed joints, the majority of cracks occurred at the bottom pad on the PCB. The prevailing crack sites occurring on PCB pads is consistent with industry experience for drop tests [3], and can be attributed to the shock wave traveling through the PCB [4]. Combinations of alloys and profiles appear to have an insignificant effect on the failure site.
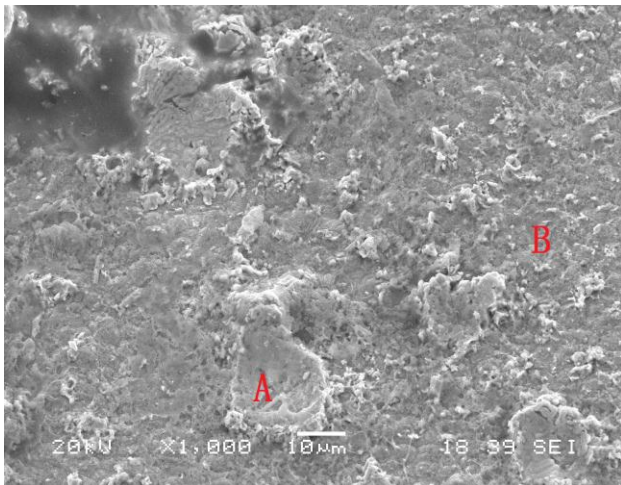

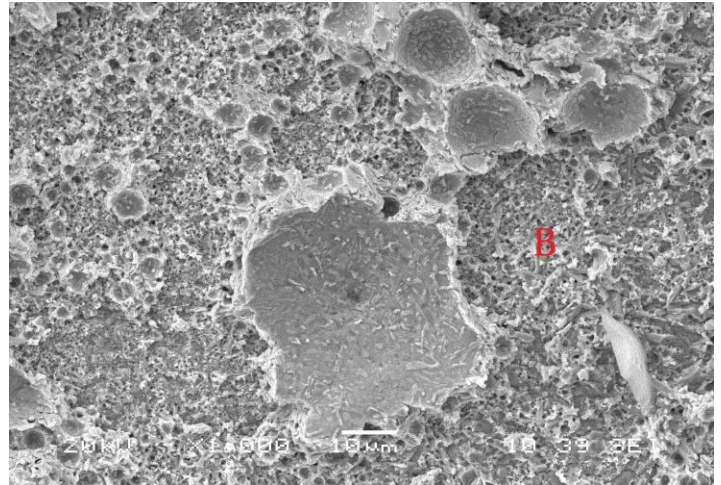**Figure 11** SEM 1000X picture of BiSnAG-105 LT ruptured surface on pad.

Figure 12 SEM 1000X picture of BiSnAG-105 HT ruptured surface on pad.

Table 7 Results of drop test for various combinations of alloys and profile.

Paste/Ball Profile	Drop no. to failure		Crack % at bottom pad	
	Ave	STD DEV	% of Joints	STD DEV %
BiSnAg/BiSnAg LT	1	0	76.9	12.1
BiSnAg/BiSnAg HT	1	0	96.8	1.6
BiSnAg/105 LT	1	0	100	0
BiSnAg/105 HT	1	0	96	2
BiSnAg/305 LT	1	0	100	0
BiSnAg/305 HT	1	0	97.4	2.5
105/105 HT	38.1	9.9	83.9	11.7
105/305 HT	24.5	4.3	83.6	10.9
305/305 HT	2.9	0.8	90.5	5.7
305/105 HT	26	9.6	86.5	12.2
SnPb/SnPb MT	38.9	11.3	69.8	11.9
305/BiSnAg LT	1	0	NA	NA
305/BiSnAg HT	1	0	22.7	13.9
105/BiSnAg LT	1	0	77.1	12.5
105/BiSnAg HT	1	0	93.4	2.1

Presence of voids have been reported to affect the mechanical properties of joints [5] and deteriorate the strength, ductility, creep, and fatigue life [6,7], due to the growth in voids, which could coalesce to form ductile cracks and consequently lead to failure. In this study, the effect of voiding on elongation at break (see Fig. 13), shear strength (see Fig. 14), and drop number to failure (see Fig. 15) are examined. Essentially, no correlation can be identified.

However, when closely examining Fig. 15, the solder composition appears to have a strong influence on drop number. All Bi-containing systems have a very low drop number, and all the non-Bi-containing systems have a higher drop number, as detailed in Table 8. This suggests that voiding is a secondary factor in drop test performance.

Fig. 15 shows that no trend can be discerned between shear strength and drop number to failure. Fig. 16 plots the elongation at break against drop number to failure. Results show that drop number increases with increasing elongation at break of solder bumps.

Discussion

1. Volume Effect

In this study, the solder volume ratio of solder paste to solder ball is 1/9. For some fine pitch CSP or WLCSP assemblies, the ratio may be higher, such as 1/3 or 1/4. The higher ratio of paste volume in the joints may aggravate voiding behavior for SAC-BiSnAg system, since the high melting SAC paste may persist long during reflow with molten BiSnAg ball on top, thus result in more voiding due to melting sequence factor.
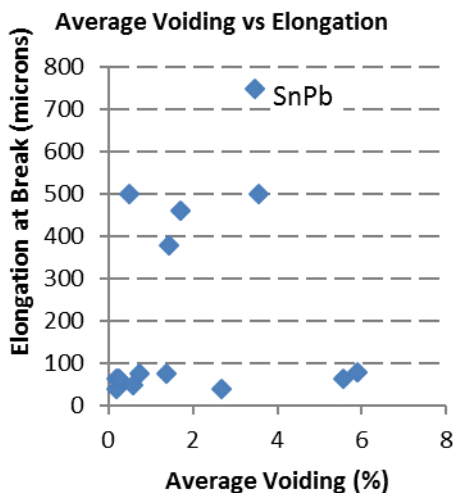
Figure 13 Effect of voiding on elongation at break.
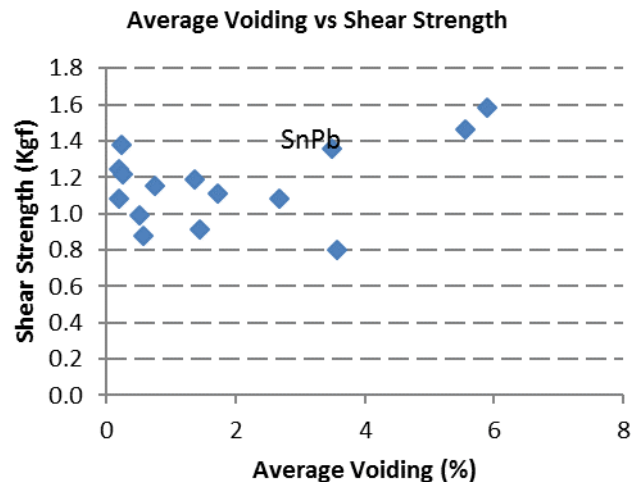
Figure 14 Effect of voiding on shear stress.
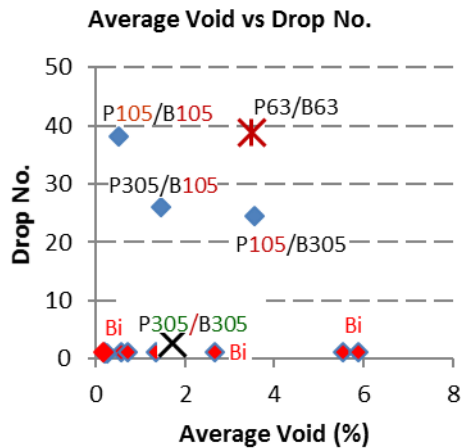
Figure 15 Relationship between average void and drop number to failure for various combinations of alloys and profiles.
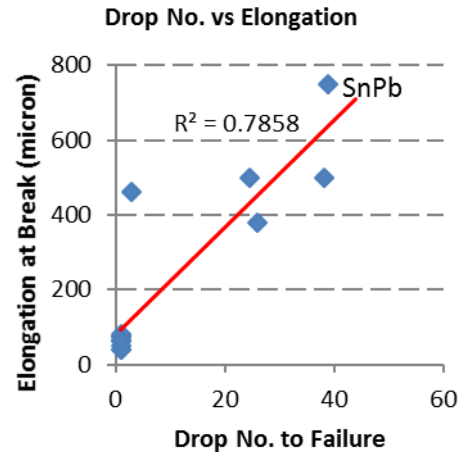

Figure 16 Effect of elongation at break on drop number.

2. Thermal Fatigue Life Prospect

Addition of Bi to Sn-based solder typically results in an increase in hardness through solution hardening mechanism. This may cause a slower creep rate and possibly a longer thermal fatigue life. In other words, although Bi-containing solder joint may suffer poor drop reliability for portable devices, it may have advantage on thermal fatigue reliability. This is attractive for stationed devices requiring a high thermal fatigue reliability but having concerns about thermal damage at assembly.

Conclusion

Low melting 57Bi42Sn1Ag (BiSnAg) was explored for replacing SAC solders as a low-cost solution. In this study, BGAs with SAC105, SAC305, or BiSnAg balls were assembled with SAC105, SAC305 or 57Bi42Sn1Ag solder paste, and the joint mechanical strength, drop test performance, and voiding performance were evaluated against the reflow profile. SnPb was included as control. The findings are:

1. The microstructure of solder joints showed that, among all of the combinations, only BiSnAg-105 LT and BiSnAg-305 LT exhibited well-distinguishable alloy regions. For SAC-BiSnAg systems, Sn-dendrites were noticeable at LT, while Ag3Sn needles developed at HT. The joints were homogeneous for the rest of the combinations.

2. In the shear test, all combinations involving BiSnAg solder were brittle, regardless of the Bi alloy location and reflow profile, as evidenced by stress-strain curves and morphology of the ruptured surface. The strong influence of Bi on the rupture site may be caused by the stiffening effect of solder due to the homogenized presence of Bi in the joint. With the stiffened solder body, the brittle IMC interface became the weakest link upon shearing, although the brittle BiSn crystalline structure also contributed to the rupture.

3. In the drop test, consistent with shear test results, all Bi-containing solder joints performed poorly compared to Bi-free systems. Drop number increased with increasing elongation at break of solder bumps measured at shear test.

4. Voiding was affected by flux chemistry. It was reduced by a low alloy homogenization temperature and solid top factor, but was increased by a low surface tension factor, melting sequence factor, overheating factor, and a wide pasty range factor. Compared to SAC or SnPb systems, BiSnAg system is low in voiding if reflowed at LT. In this study, voiding had an insignificant effect on shear strength and drop test performance.
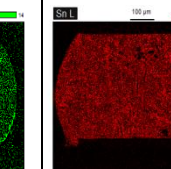
Acknowledgement
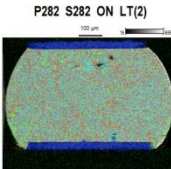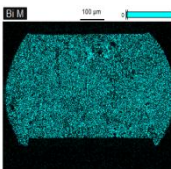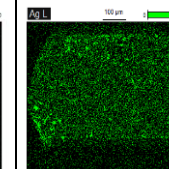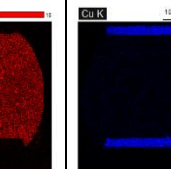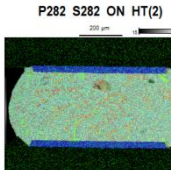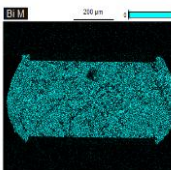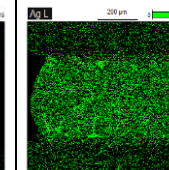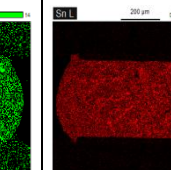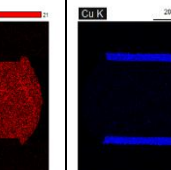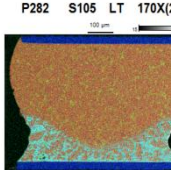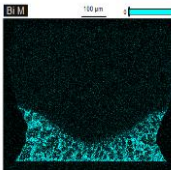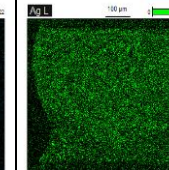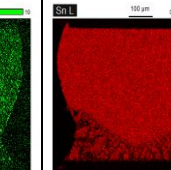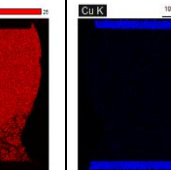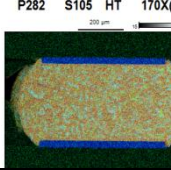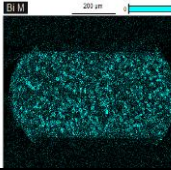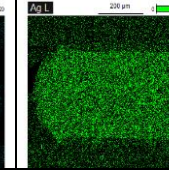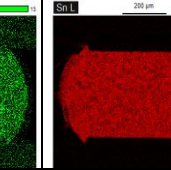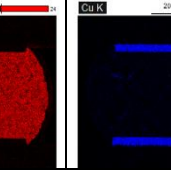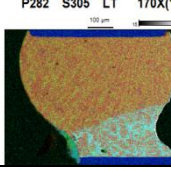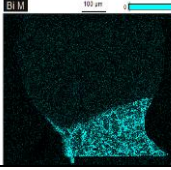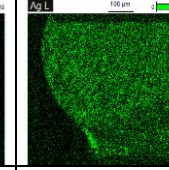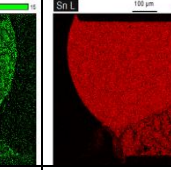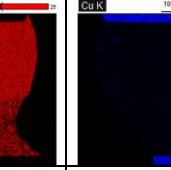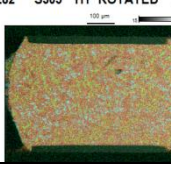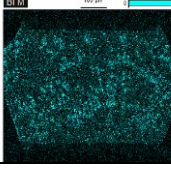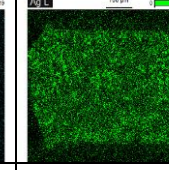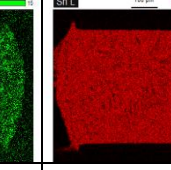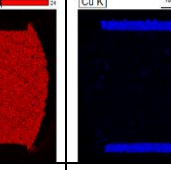
References

1. Yan Liu, Derrick Herron, Joanna Keck, and Ning-Cheng Lee, "Voiding Behavior in Mixed Solder Alloy Systems", SMTAI, Orlando, FL, October 14-18, 2012

2. Arnab Dasgupta, Benlih Huang, and Ning-Cheng Lee, "Effect of Lead-Free Alloys on Voiding at Microvia", Apex, Anaheim, CA, Feb. 23-27, 2004

3. P. T. Vianco, J. M. Grazier, J. A. Rejent, and A. C. Kilgo, Sandia National Laboratories; F. Verdi and C. Meola, ACI Technologies, Inc." Temperature Cycling of Pb-free and Mixed Solder Interconnections Used on a Package-on-Package Test Vehicle", SMTAI, p.22-34, Orlando, FL, USA, Oct. 24-28, 2010

4. R. Wayne Johnson, Yueli Liu, Guoyun Tian, Shyam Gale, and Pradeep Lall (Auburn University), "Assembly and Drop Test Reliability of Lead-Free CSPs", 2003

5. D. T. Novick, "A Metallurgical Approach to Cracked Joints," Welding J. Res. Suppl. 52, (4), 154S-158S (1973).

6. A. der Marderosian and V. Gionet, "The Effects of Entrapped Bubbles in Solder for The Attachment of Leadless Ceramic Chip Carriers'" in Proc. 21st IEEE International Reliability Physics Symposium, Phoenix, Arizona, pp.235-241 (1983).

7. V. Tvergaard, "Material Failure by Void Growth to Coalescence," in Advances in Applied Mechanics, Vol. 27 (1989), Pergamon Press, pp. 83-149.

Appendix A Elemental mapping for various alloy and reflow profile combinations

Paste-Ball Profile	SEM	Bi	Ag	Sn	Cu
BiSnAg-BiSnAg LT					
BiSnAg-BiSnAg HT					
BiSnAg-105 LT					
BiSnAg-105 HT					
BiSnAg-305 LT					
BiSnAg-305 HT					
Paste-Ball Profile	SEM	Bi	Ag	Sn	Cu
105-105 HT					

Sample	SEM	Bi M	Ag L	Sn L	Cu K
105-305 HT	P105 S305 ON HT(2) 200 µm		Ag L 200 µm	Sn L 200 µm	Cu K 200 µm
305-305 HT	P305 S305 ON HT (2) 200 µm		Ag L 200 µm	Sn L 200 µm	Cu K 200 µm
305-105 HT	P305 S105 ON HT(2) 200 µm		Ag L 200 µm	Sn L 200 µm	Cu K 200 µm
SnPb-SnPb MT	B2 P2 4MIN(3) 200 µm			Sn L 200 µm	Cu K 200 µm
305-BiSnAg LT	P305 S282 LT(2) 200 µm	Bi M 200 µm	Ag L 200 µm	Sn L 200 µm	Cu K 200 µm
305-BiSnAg HT	P305 S282 HT A 150X 200 µm	Bi M 200 µm	Ag L 200 µm	Sn L 200 µm	Cu K 200 µm
105-BiSnAg LT	P105 S282 170X(2) 100 µm	Bi M 100 µm	Ag L 100 µm	Sn L 100 µm	Cu K 100 µm
105-BiSnAg HT	P105 S282 HT 170X(100 µm	Bi M 100 µm	Ag L 100 µm	Sn L 100 µm	Cu K 100 µm